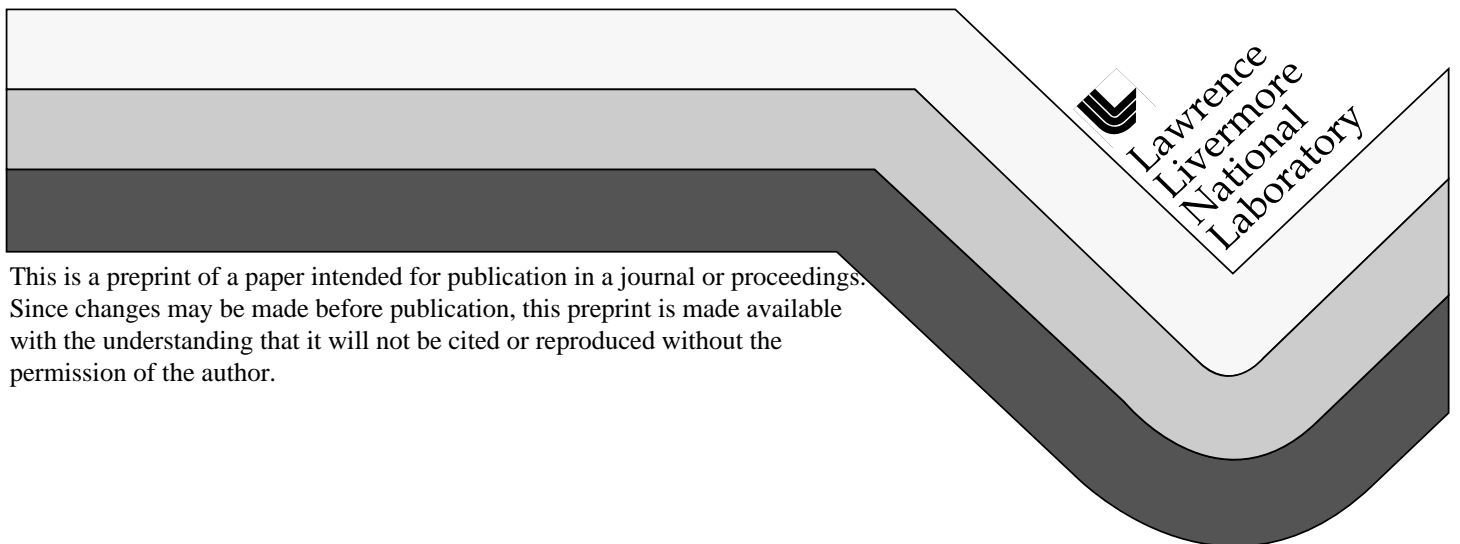


Energy and Momentum Conserving Algorithms for Rigid Body Contact

M.A. Puso
E. Zywicz

This paper was prepared for submittal to the
International Conference on
Computational Engineering Science
Atlanta, Georgia
October 6-9, 1998

April 9, 1998



This is a preprint of a paper intended for publication in a journal or proceedings.
Since changes may be made before publication, this preprint is made available
with the understanding that it will not be cited or reproduced without the
permission of the author.

DISCLAIMER

This document was prepared as an account of work sponsored by an agency of the United States Government. Neither the United States Government nor the University of California nor any of their employees, makes any warranty, express or implied, or assumes any legal liability or responsibility for the accuracy, completeness, or usefulness of any information, apparatus, product, or process disclosed, or represents that its use would not infringe privately owned rights. Reference herein to any specific commercial product, process, or service by trade name, trademark, manufacturer, or otherwise, does not necessarily constitute or imply its endorsement, recommendation, or favoring by the United States Government or the University of California. The views and opinions of authors expressed herein do not necessarily state or reflect those of the United States Government or the University of California, and shall not be used for advertising or product endorsement purposes.

Energy and Momentum Conserving Algorithms for Rigid Body Contact¹

Michael Puso

Edward Zywick

The University Of California
Lawrence Livermore National Laboratory

Summary

Energy-momentum conserving methods are developed for rigid body dynamics with contact. Because these methods are unconditionally stable, they are not time step dependent and, hence, are well suited for incorporation into structural mechanics finite element codes. Both penalty and Lagrange multiplier methods are developed herein and are the extension of the energy-momentum conserving integration schemes for rigid bodies given by Simo and Wong [1].

Introduction

The rigid material idealization is often exploited in finite element analysis to save computational time since rigid materials do not require constitutive evaluations and vastly reduce the number of degrees of freedom in the problem. Yet, the algorithms for integrating the equations of motion of these rigid bodies are more complicated than those for deformable solid elements due to presence of angular momentum. Furthermore, in an explicit setting, it is difficult to evaluate a critical time step for the rigid material unlike the deformable materials. In an implicit setting, the conventional integration algorithms and contact methods don't guarantee stability and can often gain energy in a dynamics problem. In this work we extend the implicit time integration algorithms for rigid bodies given in [1] to include the constraints and generalized forces from contact and show that the resulting formulation is energy-momentum conserving for a system of rigid bodies free of external forces. The resulting algorithms can be shown to be unconditionally stable in the energy sense [2].

We develop both Lagrange multiplier and penalty methods for versatility. The forward increment Lagrange multiplier method [3] is used with the appropriate application of contact forces/moments and an algorithmic velocity constraint to simulate elastic contact (i.e. the coefficient of restitution $e = 1$) [4]. The Lagrange multiplier method was implemented into the explicit finite element code DYNA3D [5]. We prefer the implicit rigid body dynamics algorithm in the otherwise explicit code since the iterations can be done locally and no time step constraint is imposed on the system by the rigid material. The penalty method was implemented in the implicit finite element code NIKE3D [7]. The penalty method uses an algorithmic gap given in [6] and the appropriate midstep configuration for application of forces/moments to mitigate penetration. These DYNA3D

¹ Work performed under the auspices of the U.S. Department of Energy by Lawrence Livermore National Laboratory under Contract W-7405-Eng-48.

and NIKE3D implementations are general in that they include flexible - flexible, flexible - rigid and rigid - rigid contact. Although we have included friction in our implementation, the work presented here is frictionless.

In what follows: the notion of algorithmic energy-momentum conservation is defined, the time integration methods are shown, the special contact treatment is presented and finally a few simple examples are illustrated.

Energy-Momentum Conservation

Consider the free body motion of N rigid bodies with contact. Using the midpoint rule, the discretized momentum equations for the i th body are given by:

$$\mathbf{p}_{n+1}^i - \mathbf{p}_n^i = \sum_{j=1}^{N_c} (\mathbf{f}_{n+1/2}^j)^i \Delta t \quad \mathbf{h}_{n+1}^i - \mathbf{h}_n^i = \sum_{j=1}^{N_c} (\bar{\mathbf{R}}^j)^i \times (\mathbf{f}_{n+1/2}^j)^i \Delta t \quad (1)$$

where $\mathbf{p}_n^i = M^i \mathbf{v}_n^i$ is the linear momentum, $\mathbf{h}_n^i = \mathbf{I}_n^i \cdot \boldsymbol{\omega}_n^i$ is the angular momentum, \mathbf{v} is the velocity of the center of mass, $\boldsymbol{\omega}$ is the rotation rate, M is the mass, \mathbf{I} is moment of inertia, $(\mathbf{f}^j)^i$ is the contact force on the j th node, $(\bar{\mathbf{R}}^j)^i$ is the appropriately defined moment arm measured from the center of mass to the j th node, and N_c is the number of nodal contact forces applied. Conservation of the discretized system linear and angular momentums is represented by:

$$\sum_{i=1}^N \mathbf{p}_n^i = P \quad \sum_{i=1}^N \mathbf{X}^i \times \mathbf{p}_n^i + \mathbf{h}_n^i = H \quad (2)$$

where P and H are constants and \mathbf{X} is the location of the center of mass. Energy conservation is given by:

$$T_n + U_n = E \quad \text{where} \quad T_n = \sum_{i=1}^N \mathbf{p}_n^i \cdot \mathbf{v}_n^i + \mathbf{h}_n^i \cdot \boldsymbol{\omega}_n^i \quad (3)$$

where E is some constant and U is some stored potential energy which may be non-zero when contact is made in the penalty method ($U = 0$ in the Lagrange multiplier method). In general, time stepping methods satisfy (1), but (2) and (3) are only satisfied in the limit as $\Delta t \rightarrow 0$. It remains to develop the appropriate definitions for \mathbf{f} , $\bar{\mathbf{R}}$, U and time integration rules such that the conservation laws (2) and (3) can be satisfied to some desired tolerance.

Integration Rules

The rigid body center of mass and rotation are updated using the following integration rules from Simo and Wong [1]:

$$\mathbf{X}_{n+1} = \frac{\Delta t}{2} (\mathbf{v}_{n+1} + \mathbf{v}_n) + \mathbf{X}_n \quad (4)$$

$$\mathbf{A}_{n+1} = \exp [\hat{\boldsymbol{\theta}}_{n+1}] \quad (5)$$

$$\boldsymbol{\omega}_{n+1} = \mathbf{A}_{n+1} \left(\frac{2}{\Delta t} \hat{\boldsymbol{\theta}}_{n+1} - \boldsymbol{\omega}_n \right) \quad (6)$$

$$\mathbf{I}_{n+1} = \mathbf{A}_{n+1} \mathbf{I}_n \mathbf{A}_{n+1}^T \quad (7)$$

where $\hat{\boldsymbol{\theta}}$ is the incremental rotation and $\exp [\cdot]$ is the exponential map operator which maps the incremental rotation into $\text{SO}(3)$. Solutions to linearized forms (c.f. [1],[8]) of (1) will provide the incremental displacements and rotations which are used in (4)-(7) to update the kinematics.

Contact Forces and Moments

For the penalty method, an algorithmic definition of the gap is used in place of the exact gap. In this method, the closest point projection is made at a modified configuration $\bar{\mathbf{x}}$ from which the contact normal $\bar{\mathbf{v}}$ and isoparametric coordinates $\bar{\xi}$ are calculated. The algorithmic gap is given by the recursion [6]:

$$g_{n+1}^d = g_n^d + \bar{\mathbf{v}} \cdot ((\mathbf{x}_{n+1}^s - \mathbf{x}_n^s) - (\mathbf{x}(\bar{\xi}_{n+1}^m) - \mathbf{x}(\bar{\xi}_n^m))) \quad (8)$$

where \mathbf{x}^s represents the position of the slave node and \mathbf{x}^m is the position of the closest point projection at a given time. This so called dynamic gap is a second order approximation to the actual gap. The contact forces on the slave node \mathbf{f}^s and the i th master node $(\mathbf{f}^m)^i$ are given by [6]:

$$\mathbf{f}^s = p \bar{\mathbf{v}} \quad \text{and} \quad (\mathbf{f}^m)^i = -p \bar{\mathbf{v}} N^i(\bar{\xi}) \quad (9)$$

$$\text{where} \quad p = \frac{1}{2} \frac{U_{n+1} - U_n}{g_{n+1}^d - g_n^d} \quad \text{and} \quad U = \begin{cases} k (g^d)^2 & \text{if } g < 0 \\ 0 & \text{otherwise} \end{cases} \quad (10)$$

The nodal points on both the slave and master surfaces of the rigid bodies are calculated at a modified position given by:

$$\bar{\mathbf{x}} = \frac{1}{2} (\mathbf{X}_{n+1} + \mathbf{X}_n) + \bar{\mathbf{R}}, \quad \text{where} \quad \bar{\mathbf{R}} = \frac{1}{2} \frac{\tan(|\boldsymbol{\theta}_{n+1}|/2)}{|\boldsymbol{\theta}_{n+1}|/2} (\mathbf{R}_{n+1} + \mathbf{R}_n), \quad (11)$$

\mathbf{X} is the position of the center of mass, \mathbf{R} is the position to the node from the center of mass and $\boldsymbol{\theta}$ is the compound rotation. From the nodal positions given by (11), the contact normal $\bar{\mathbf{v}}$ and the moment arm $\bar{\mathbf{R}}$ are calculated. As shown in Appendix A, use of this modified position along with the penalty forces from (9)-(10) provides system momentum and energy conservation.

In the forward increment Lagrange multiplier method, a "predictor" step is taken in which no contact forces are applied. From the predictor step nodal positions, slave and master facet pairs are identified. The moment arms \mathbf{R}_p and contact normals $\bar{\mathbf{v}}$ are calculated by closest point projection in the predicted state. The contact force is now:

$$\mathbf{f} = \lambda \bar{\mathbf{v}} \quad (12)$$

where λ is the unknown Lagrange multiplier. The following algorithmic moment arms for the slave and master nodes are used to conserve angular momentum:

$$\bar{\mathbf{R}}^s = \mathbf{R}_p^s + ((\mathbf{X}_n^s - \mathbf{X}_n^m) + (\mathbf{R}_p^s - \mathbf{R}_p^m)) / 2 \quad \bar{\mathbf{R}}^m = \mathbf{R}_p^m - ((\mathbf{X}_n^s - \mathbf{X}_n^m) + (\mathbf{R}_p^s - \mathbf{R}_p^m)) / 2 \quad (13)$$

The Lagrange multiplier is calculated such that the following gap velocity constraint is enforced:

$$\bar{\mathbf{v}} \cdot (\Delta \mathbf{v}^m - \Delta \mathbf{v}^s) = 0 \quad (14)$$

where $\Delta \mathbf{v}$ is the algorithmic velocity jump of the slave/master node from time n to $n+1$, and is given by:

$$\Delta \mathbf{v} = 1/2 (\mathbf{v}_{n+1} + \mathbf{v}_n) + (\exp^T(\hat{\boldsymbol{\theta}}_{n+1}) \boldsymbol{\omega}_{n+1} + \boldsymbol{\omega}_n) \times \bar{\mathbf{R}} \quad (15)$$

Here \mathbf{v} is the velocity of the center of mass. By substituting (15) and (6) into (A1), it can be shown that the method conserves energy algorithmically. In the limit as $\Delta t \rightarrow 0$, the rotation $\exp(\hat{\boldsymbol{\theta}})$ tends toward the identity matrix and the continuum result is recovered for an elastic collision [4].

The above algorithm is embedded in a nonlinear conjugate gradient algorithm to solve for the updated position and Lagrange multipliers. The conjugate gradient method employs constraint planes which enforce the Kuhn Tucker complementary conditions for the contact forces and gaps. The method used is described in detail in references [8] and [9].

Examples

The penalty method was particularized to solve problems involving rigid spherical contact. In doing so, spheres can roll smoothly against contact surfaces. In the first example (Figure 1), a 0.274 kg solid ball, radius 1 m , is placed within a 0.743 kg spherical shell, inner radius 9 m (Fig. 1). Initially, the center of mass is at $(0,0,2)$ for the solid ball and $(0,0,10)$ for the shell. The solid ball is given an initial velocity of 1 m/s in the y direction such that the inner ball rolls smoothly in the y - z plane. Because the system is entirely free, linear and angular momentum of the system is conserved (see Fig. 2). The relative error for system kinetic energy, defined as $T / T_o - 1$, reaches a maximum 3×10^{-9} while the relative error in x angular momentum (Figure 2) reaches 8.8×10^{-11} . The penalty stiffness was 10,000 and it is noted that some of the energy in the system is potential.

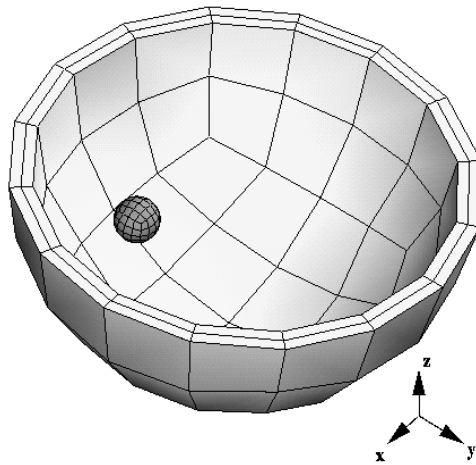


Figure 1. Rigid ball in spherical shell.

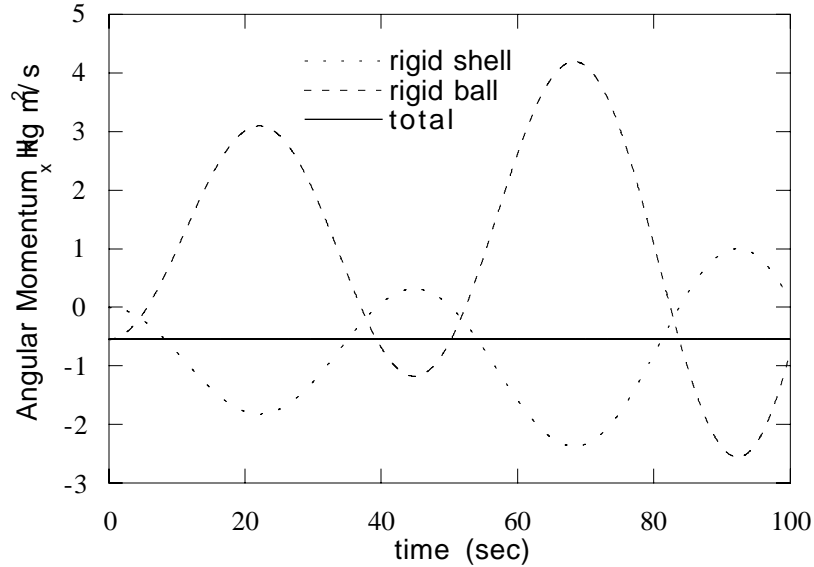


Figure 2. x angular momentum for rigid ball and spherical shell.

In the next example, the Lagrange multiplier method in DYNA3D is used to model a moving 1 m long rod confined within a rigid cube (Figure 3). The unconstrained cube, initially stationary, measures 2 m by 2 m by 2 m and is 0.1 m thick. The rod, initially centered within the cube and coincidental with the x -axis is made from five collinear beam elements, and its cross section measures 0.1 m by 0.1 m . It has an initial velocity of $\dot{\mathbf{x}} = (50, 2, 0)^T$ m/s and $\dot{\boldsymbol{\theta}} = (0, 40, 0)^T$ rad/s . Both materials have a density of 7.0×10^{-4} kg/m^3 . The analysis is run for 10 sec with a fixed time step size of 1×10^{-6} sec . During the 10^7 steps the rod impacts the cube 447 separate times. The relative error for system kinetic energy reaches a peak value of 9.46×10^{-11} while the relative error in y angular momentum reaches 2.86×10^{-5} . All other error is within machine tolerance.

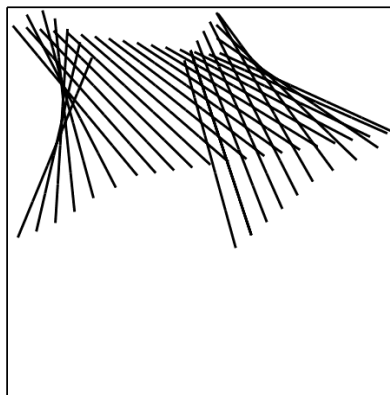


Figure 3. Rigid stick in rigid box.

References

1. Simo, J. C. and Wong, K. K. (1991), "Unconditionally Stable Algorithms for Rigid Body Dynamics that Exactly Preserve Energy and Momentum", Int. J. Num. Meth. Eng. Vol. 31.
2. Richtmyer, R. D. and Morthon K. W. (1967), Difference Methods for Initial Value Problems, InterScience.
3. Carpenter, N. J., Taylor, R. L. and Katona, M. G. (1991), "Lagrange Constraints for Transient Finite Element Surface Contact", Int. J. Num. Meth. Eng. Vol. 32.
4. Kane, T. R. and Levinson, D. A. (1985), Dynamics: Theory and Applications, McGraw Hill.
5. Whirley, R. G. and Engelmann, B. E. (1993), "DYNA3D: User Manual", Report UCRL-MA-107254, Lawrence Livermore National Laboratory.
6. Armero, F. and Petocz, E. (1997), "Formulation and Analysis of Conserving Algorithms for Dynamic Contact Impact Problems", Report UCB/SEMM-96/10, University of California, Berkeley.
7. Maker, B. N. (1995), "NIKE3D: User Manual", Report UCRL-MA-105268, Lawrence Livermore National Laboratory.
8. Zywicz, E. and Puso, M. A., (1997), "A General Predictor-Corrector Solver for Explicit Finite-Element Contact", Report UCRL-JC-128410, Lawrence Livermore National Laboratory.
9. Sha, D., Tamma, K. K. and Neal, M. O. (1996), "Robust Explicit Computational Developments and Solution Strategies for Impact Problems Involving Friction", Int. J. Num. Meth. Eng. Vol. 39.

Appendix A

Energy Conservation for Penalty Method:

The change in algorithmic kinetic energy from time n to $n + 1$ is found by premultiplying the translational and angular momentum equations in (1) by the incremental displacement $\mathbf{X}_{n+1} - \mathbf{X}_n$ and rotation $\boldsymbol{\theta}_{n+1}$, respectively, and adding the contributions to give:

$$\begin{aligned} T_{n+1} - T_n &= M (\mathbf{v}_{n+1})^2 - M (\mathbf{v}_n)^2 + \boldsymbol{\omega}_{n+1} \cdot \mathbf{I}_{n+1} \boldsymbol{\omega}_{n+1} - \boldsymbol{\omega}_n \cdot \mathbf{I}_n \boldsymbol{\omega}_n \\ &= \sum_{j=1}^{N_c} (\mathbf{f}_{n+1/2}^i)^j \cdot (\mathbf{X}_{n+1} - \mathbf{X}_n + \boldsymbol{\theta}_{n+1} \times \bar{\mathbf{R}}^j) \end{aligned} \quad (\text{A1})$$

where the identity $(\mathbf{I} - \exp[\boldsymbol{\theta}]) \cdot \boldsymbol{\theta} = 0$ is used. Using the following identity:

$$\frac{\tan(|\boldsymbol{\theta}_{n+1}|/2)}{|\boldsymbol{\theta}_{n+1}|/2} \boldsymbol{\theta} \times \frac{1}{2} (\mathbf{R}_{n+1} + \mathbf{R}_n) = (\mathbf{R}_{n+1} - \mathbf{R}_n) \quad (\text{A2})$$

along with (11) in (A1) gives:

$$T_{n+1} - T_n = \sum_{j=1}^{N_c} (\mathbf{f}_{n+1/2}^i)^j \cdot ((\mathbf{X}_{n+1} + \mathbf{R}_{n+1}^j) - (\mathbf{X}_n + \mathbf{R}_n^j)) \quad (\text{A3})$$

Without loss of generality, it is shown that contact between two rigid bodies at a single master-slave pair conserves energy. Using (A3), (9) and (10) the total algorithmic potential energy from both rigid bodies can be shown to be:

$$\begin{aligned} T_{n+1} - T_n &= p \bar{\mathbf{v}} \cdot \left[(\mathbf{X}_{n+1}^s + \mathbf{R}_{n+1}^s) - (\mathbf{X}_n^s + \mathbf{R}_n^s) - \right. \\ &\quad \left. \sum_{j=1}^4 (N^j(\boldsymbol{\xi}) \cdot ((\mathbf{X}_{n+1}^m + \mathbf{R}_{n+1}^{mj}) - (\mathbf{X}_n^m + \mathbf{R}_n^{mj}))) \right] \end{aligned} \quad (\text{A4})$$

where the master facet is assumed to have four nodes. Now using the definition for the algorithmic gap in (8) and the contact pressure (10) in (A4), the change in kinetic energy is shown to be the change in potential energy of contact:

$$T_{n+1} - T_n = U(g_{n+1}^d) - U(g_n^d) \quad (\text{A5})$$

Conservation of Momentum for Penalty Method:

Linear momentum is conserved by definition in (9). Without loss of generality, the total algorithmic angular momentum is shown to be conserved for two rigid bodies in contact at a single master-slave pair such that

$$\begin{aligned} \mathbf{H}_{n+1} - \mathbf{H}_n &= (\mathbf{X}_{n+1}^s \times M^s \mathbf{v}_{n+1}^s + \mathbf{X}_{n+1}^m \times M^m \mathbf{v}_{n+1}^m + \mathbf{I}_{n+1}^s \boldsymbol{\omega}_{n+1}^s + \mathbf{I}_{n+1}^m \boldsymbol{\omega}_{n+1}^m) - \\ &\quad (\mathbf{X}_n^s \times M^s \mathbf{v}_n^s + \mathbf{X}_n^m \times M^m \mathbf{v}_n^m + \mathbf{I}_n^s \boldsymbol{\omega}_n^s + \mathbf{I}_n^m \boldsymbol{\omega}_n^m) \end{aligned} \quad (\text{A6})$$

Using (1), (10), (11) and the result $(\mathbf{X}_{n+1} - \mathbf{X}_n) \times M(\mathbf{v}_{n+1} + \mathbf{v}_n) = 0$ in (A6) with some algebraic manipulation gives:

$$\mathbf{H}_{n+1} - \mathbf{H}_n = (\bar{\mathbf{x}}^s - \bar{\mathbf{x}}(\boldsymbol{\xi})^m) \times p \bar{\mathbf{v}} \quad (\text{A7})$$

Because the closest point projection is made in the modified position given by (11), the result $\bar{\mathbf{x}}^s - \bar{\mathbf{x}}(\boldsymbol{\xi})^m = g \bar{\mathbf{v}}$ holds and the change of momentum in (A7) vanishes.

Technical Information Department • Lawrence Livermore National Laboratory
University of California • Livermore, California 94551

